

# Designer magnetic superatoms

J. Ulises Reveles<sup>1</sup>, Peneé A. Clayborne<sup>1</sup>, Arthur C. Reber<sup>1</sup>, Shiv N. Khanna<sup>1\*</sup>, Kalpataru Pradhan<sup>2</sup>, Prasenjit Sen<sup>2</sup> and Mark R. Pederson<sup>3</sup>

**The quantum states in metal clusters are grouped into bunches of close-lying eigenvalues, termed electronic shells, similar to those of atoms. Filling of the electronic shells with paired electrons results in local minima in energy to give stable species called magic clusters. This led to the realization that selected clusters mimic chemical properties of elemental atoms on the periodic table and can be classified as superatoms. So far the work on superatoms has focused on non-magnetic species. Here we propose a framework for magnetic superatoms by invoking systems that have both localized and delocalized electronic states, in which localized electrons stabilize magnetic moments and filled nearly-free electron shells lead to stable species. An isolated  $\text{VCs}_8$  and a ligated  $\text{MnAu}_{24}(\text{SH})_{18}$  are shown to be such magnetic superatoms. The magnetic superatoms' assemblies could be ideal for molecular electronic devices, as the coupling could be altered by charging or weak fields.**

One of the exciting moments of cluster science was the introduction of the concept that selected stable clusters could mimic the chemical behaviour of elemental atoms<sup>1–10</sup>. The clusters, called superatoms, form a third dimension of the periodic table, and could serve as the building blocks of nanomaterials with desired properties. The basic idea of superatoms rests on the premise that the nature of the valence electronic spectrum and the associated chemical valence of clusters may be analogous to those of atoms<sup>1,5–8</sup>. For metal clusters, this analogy can be seen through electronic shells in a confined nearly-free electron (NFE) gas<sup>11–14</sup> in which the quantum confinement results in an electronic level sequence  $1S^21P^61D^{10}$ , much like those in an atom (but with a different combination of quantum numbers). Throughout this paper, lower case letters (*s*, *p*, *d*, ...) are used to denote electronic levels in atoms and upper case letters (*S*, *P*, *D*, ...) to denote shells of electrons in a confined NFE gas. That aluminium has three valence electrons per atom led to the idea that an  $\text{Al}_{13}$  cluster with a  $1P^5$  valence state should have the high electron affinity that halogens have. The theoretical calculations<sup>1</sup> and the subsequent experiments<sup>3,6,15</sup> confirmed an electron affinity close to that of a chlorine atom. Further work<sup>6</sup> revealed behaviour like that of halogen atoms when combined, in particular, with iodine atoms. Over the past few years, several clusters, including  $\text{Al}_{13}$ ,  $\text{BAI}_{12}$ ,  $\text{Al}_{14}$ ,  $\text{Al}_7^-$  and  $(\text{As}_7^{3-})$  have been found to mimic the behaviours of halogen, alkaline earth and multivalent species, and of polyvalent atoms<sup>1,2,5–8</sup>, and hence belong to the superatom family. It was proposed recently that the superatom concept can also be extended to metal clusters, such as  $\text{Au}_n$ , ligated with thiolate (SR complex) and other ligands<sup>16–18</sup>. The ligands that surround the metallic core act to withdraw electrons from the metal, which leads to stable species when the electron count corresponds to a filled electronic shell, as in stable free clusters.

The existing idea of superatoms hinges on acquiring stability through closed electronic shells of paired electrons. Consequently, it is restricted to non-magnetic species because magnetism requires unpaired species. Here we propose that magnetic superatoms can be realized if electronic shells of the valence pool have localized as well as diffuse subspaces. One way to accomplish this is to consider

composite systems with some atoms that have relatively localized orbitals (for example, *d* or *f*) with a large separation between spin-up and -down levels as well as diffuse valence orbitals and others that have NFEs. Such systems would acquire the magnetic moment via orbitals that are localized at the atomic sites and do not overlap significantly as atoms are assembled, although the nearly-free diffuse *SP* orbitals could impart stability through electronic shells of diffuse states. In this work, we demonstrate this intriguing possibility with free clusters composed of a vanadium atom surrounded by alkali atoms and with a ligated  $\text{MnAu}_{24}(\text{SH})_{18}$  cluster. In particular, a  $\text{VCs}_8$  cluster is shown to have a partially filled *d* subshell and a filled delocalized *SP* electronic supershell. The closest atomic analogue is manganese, which has an electronic configuration of  $d^5s^2$  with a *d* subshell of five unpaired electrons and a closed atomic *s* shell of two electrons. The analogy extends to dimers and trimers, in which analogues of changes in magnetic coupling in  $\text{Mn}_n$  (refs 19–21) on charging are found in superatom clusters.

The behaviour of vanadium atoms in bulk alkali hosts that provide 'band-free' conduction electrons has been the subject of several experimental investigations. Vanadium is non-magnetic in the solid phase, but vanadium atoms can have a maximum moment of  $3\mu_B$  (Bohr magneton) per atom (with three electrons occupying the *d* sub-band). Small vanadium clusters are non-magnetic<sup>22</sup>. The anomalous Hall-effect measurements on thin films of sodium, potassium and caesium that contain vanadium impurities indicate large atomic moments of 6.6–7.0  $\mu_B$  per atom for sodium and potassium, and of 4  $\mu_B$  for caesium films<sup>23,24</sup>. The presence of large magnetic moments was confirmed by theoretical studies of vanadium impurities in alkali hosts using a supercell approach, although the magnitude of the calculated moment was smaller than that observed experimentally<sup>25</sup>. These large magnetic moments resulted from the filled majority *d* states in a vanadium atom, whereas the minority *d* states are above the Fermi energy<sup>26</sup>. For clusters, this provides a unique opportunity to witness the effects of electron shells on stability, once the majority *d* states of the vanadium atom are filled by the initial *s* electrons of the alkali atoms. This separation between the filled *d* subshell and the electronic stability that originates largely in the NFE *SP* band is the key to the design of magnetic superatoms.

<sup>1</sup>Department of Physics, Virginia Commonwealth University, Richmond, Virginia 23284, USA, <sup>2</sup>Harish-Chandra Research Institute, Chhatnag Road Jhansi, Allahabad 211019, India, <sup>3</sup>Naval Research Laboratory, Center for Computational Materials Science, Washington DC 20375, USA. \*e-mail: snkhanna@vcu.edu

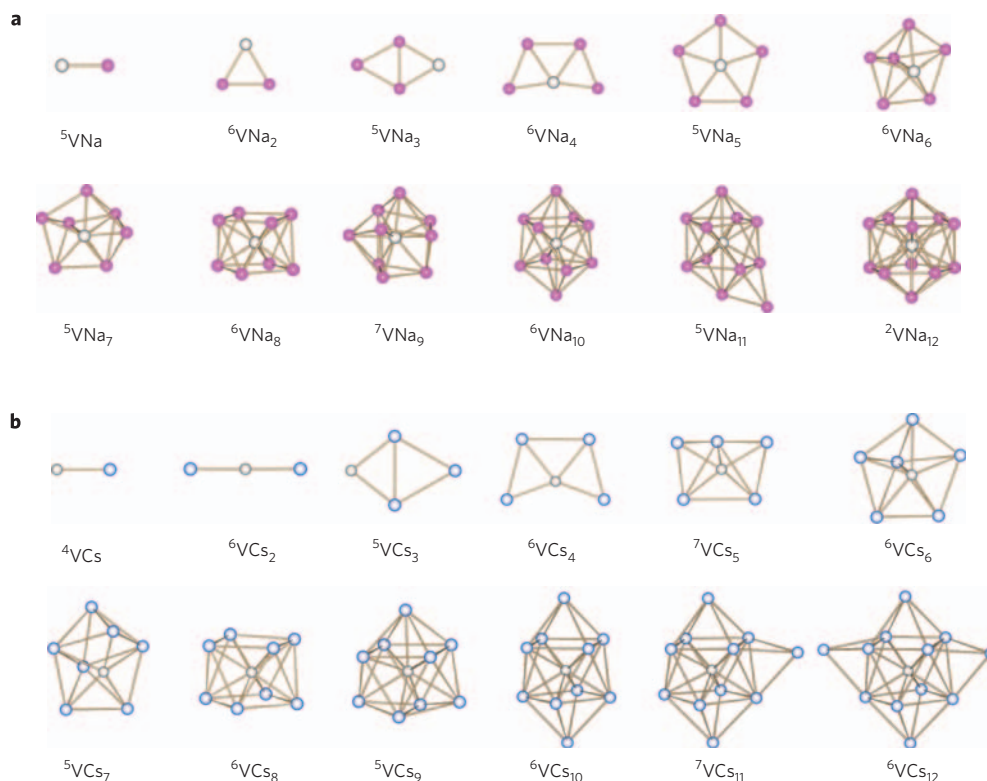


**Figure 1 | Ground-state geometries of  $VNa_n$  and  $VC_s_n$  clusters.** **a**,  $VNa_n$  ( $n=1$ –12) clusters. **b**,  $VC_s_n$  ( $n=1$ –12) clusters. The superscripts indicate spin multiplicity. Red, blue and grey circles represent sodium, caesium and vanadium atoms, respectively.

## Results and discussion

The electronic shells in metal clusters were first established from the mass spectra of  $Na_n$  clusters<sup>11</sup>. To explore any shell effects, we therefore probed the stability and magnetic moments of  $VNa_n$  clusters that contained 1–12 sodium atoms. Figure 1a shows the geometric structure of the ground-state clusters. The successive sodium atoms surround the central vanadium site, and the structure of  $VNa_8$  is a vanadium atom surrounded by a square antiprism of eight sodium atoms. The structure evolves towards a compact icosahedral shape as the number of sodium atoms is increased to 12. The quantity of interest is the change in binding energy as successive sodium atoms are added, and the progression of the spin magnetic moment. The change in binding was monitored through incremental binding energy,  $\Delta E_n$ , calculated using equation (1).

$$\Delta E_n = E(Na) + E(VNa_{n-1}) - E(VNa_n) \quad (1)$$

Here,  $E(Na)$ ,  $E(VNa_{n-1})$  and  $E(VNa_n)$  are the total energies of a sodium atom,  $VNa_{n-1}$  cluster and  $VNa_n$  cluster, respectively.  $\Delta E_n$  represents the gain in energy as a sodium atom is added to the preceding  $VNa_{n-1}$  size and was the hallmark of the enhanced stability in pure  $Na_n$  clusters. Figure 2a shows  $\Delta E_n$  as a function of  $n$ , with a distinct maximum at  $VNa_8$ . As the electronic structure of a vanadium atom is  $d^3s^2$ , the addition of eight sodium atoms creates a valence pool of ten  $sp$  electrons and, ordinarily, this does not correspond to a magic species. The situation here is different because a vanadium atom has a partially filled  $d$  subshell. As the alkali is added the initial electrons are used to fill the  $d$  subshell on vanadium, which leads to an initial increase in magnetic moment from  $3.0\mu_B$  to  $5.0\mu_B$ . Once the majority  $d$  subshell is complete, the remaining electrons occupy states of the delocalized electrons, which leads to oscillations of the total moment between 4 and  $5\mu_B$  (see Fig. 2c), depending on whether the cluster

has an odd or even number of  $SP$  electrons. A  $VNa_8$  cluster, therefore, has a half-filled  $d$  subshell with a magnetic moment of  $5\mu_B$  and the remaining electrons form a filled shell of  $1S^21P^6$  electrons, which leads to a stable species.

Figure 3 shows the one-electron energy levels and molecular orbital isosurfaces of  $VNa_8$  and confirms this picture. The atomic composition of the levels denotes a group of five levels with marked  $d$  character from the vanadium atom, and the  $d$  unoccupied states lie 0.87 eV above these levels. At the same time, eight energy levels of  $s$  character from the vanadium atom and  $s$  and  $p$  character from the sodium atoms account for the closed shell configuration  $1S^21P^6$ . Further evidence of this picture is provided by an examination of the gap between the highest occupied molecular orbital (HOMO) and the lowest unoccupied molecular orbital (LUMO). The HOMO–LUMO gap in  $VNa_8$  was found to be 0.69 eV, larger than at any other cluster size (see Supplementary Table S1). The gap is fairly high, although smaller than in covalently bonded  $C_{60}$ , which has a gap of 1.72 eV (ref. 27). In addition to energetic stability, the magnetic state was also found to be robust, as shown from an examination of the energies of various spin states at each size. From these, we determined the energy required to attain the magnetic state closest to the ground state (this comparison is given in Supplementary Table S1). Most sizes have close-lying spin multiplets, but the closest magnetic state in  $VNa_8$  is 0.51 eV higher in energy. These results indicate that  $VNa_8$  is quite stable. With magnetic electrons localized on a vanadium site, the cluster has negligible magnetic anisotropy, which makes it paramagnetic like ordinary atoms. We call it a magnetic superatom.

There are several approaches to make cluster assemblies from superatoms<sup>28–30</sup>. Clusters could be isolated in zeolite cages<sup>31</sup> or deposited on substrates. Forming nanomaterials through direct deposition on substrates, however, requires the magnetic features to be maintained throughout the assembly. Consequently, we examined the evolution of the geometry and magnetic properties as two  $VNa_8$

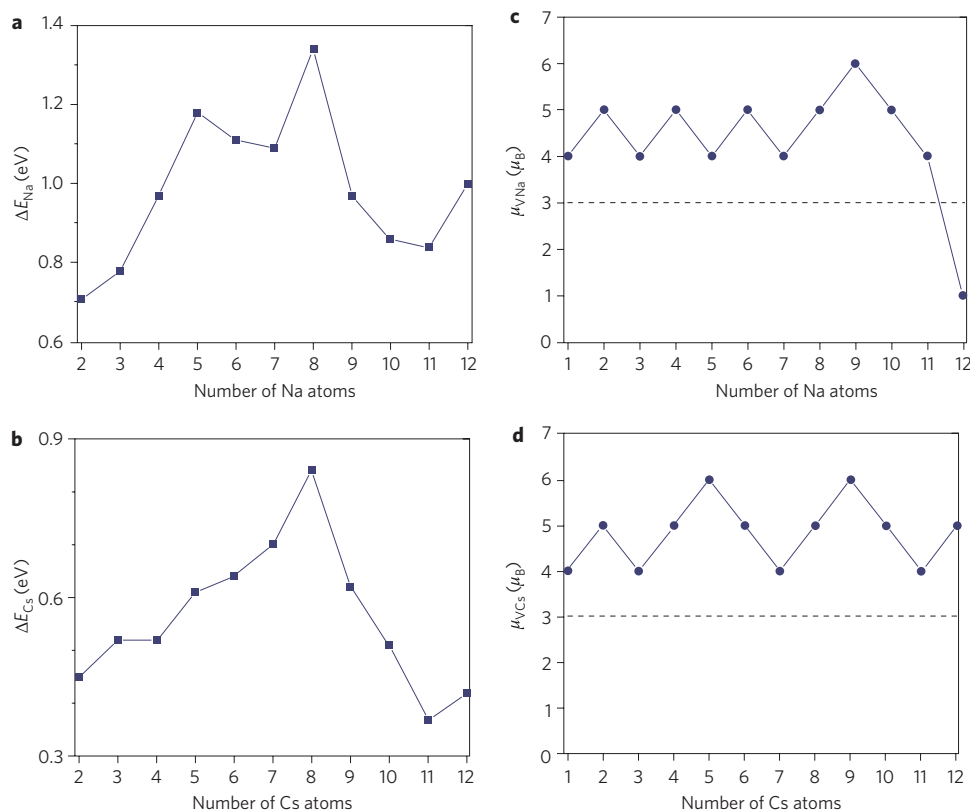


**Figure 2 | Energetic and magnetic trends of  $VNa_n$  and  $VCs_n$  clusters.** **a,b**, Variation of the gain in energy caused by alkali addition ( $\Delta E_A$ ) with  $n$  in the  $VNa_n$  (**a**) and  $VCs_n$  (**b**) clusters. **c,d**, Variation of the magnetic moments ( $\mu$ ) with  $n$  in the  $VNa_n$  (**c**) and  $VCs_n$  (**d**) clusters. The magnetic moment of the vanadium atom is also given as reference (dashed line).

clusters were brought together from an initially large separation. Figure 4a shows the ground-state geometry of the composite cluster and that the two vanadium atoms in the separate cages are able to overcome the barrier for displacing sodium atoms and so form a  $V_2$  dimer, which destroys the identity of the individual species.

There are two ways to overcome this limitation. The first is to create ionic species in which the charge could separate the individual clusters. As  $VNa_8$  is a closed-shell species,  $VNa_9$  should have an electron beyond the filled shell and hence could be linked to a halogen to form an ionic supermolecule, an idea previously used for  $Al_{13}$  clusters<sup>32</sup>. A calculation for the composite cluster made of chlorine or iodine with  $VNa_9$  demonstrated a stable species composed of a  $VNa_9^+$  cation and an  $I^-$  anion (see Supplementary Fig. S1a). Our past experience has shown that such species can form stable ionic assemblies<sup>33</sup>.

Here, however, we focus on a second possibility; namely, the use of larger alkali atoms, such as caesium, instead of sodium. Analogous studies on  $VCs_n$  clusters that contained up to 12 caesium atoms were carried out and the most stable structures are shown in Fig. 1b. The geometries at small sizes have similar arrangements to those in  $VNa_n$  and the ground state of  $VCs_8$  again presented an endohedral vanadium atom with eight caesium atoms forming a square antiprism. For clusters with more than eight caesium atoms, however, the structures of  $VCs_n$  follow a different growth pattern to that of  $VNa_n$ . As the size of caesium is larger, the inner core maintains eight caesium atoms and the additional atoms create a second shell. These patterns are similar to the differences between NaCl and CsCl structures in which the former results in face-centred cubic arrangements and the latter evolves towards a body-centred cubic arrangement. More important is the variation of  $\Delta E_n$  and the magnetic moment shown in Fig. 2b. As in case of  $VNa_n$ ,  $\Delta E_n$  shows a maxima at  $n = 8$ , which indicates enhanced

stability. The magnetic moment, however, shows a different evolution, with an oscillatory pattern up to 12 atoms as opposed to quenching of the moment in  $VNa_{12}$ . The difference is attributable to the coordination because the central vanadium has only eight nearest caesium atoms. A detailed investigation of the electronic spectrum also revealed other differences. Whereas  $VNa_8$  has a filled subshell with a majority of  $d$  electrons from vanadium, the magnetic moment in  $VCs_8$  has contributions from  $d$  and  $sp$  states mixed with  $d$ , as shown in Supplementary Fig. S2. As before, the uniqueness of the magnetic state was probed through calculations of the energy required to attain the nearest magnetic state. Supplementary Table S1 shows the energy required in  $VCs_n$  clusters, and it is higher in  $VCs_8$  than in all other clusters except  $VCs_{10}$ , which signals its spin stability. Also important is that the next-highest energy state of  $VCs_8$ , which lies 0.14 eV above the ground state, has an even higher moment of  $7\mu_B$ . In this cluster, in addition to the five unpaired  $d$  electrons of vanadium, the polarization of the  $s$  electrons of vanadium and  $s$  and  $p$  electrons of caesium increased the magnetic moment.

As the larger size of caesium leads to a first shell of only eight caesium atoms, we examined both the possibility of forming ionic species by combining it with chlorine or iodine and also the progression of the geometry and the magnetic properties as two  $VCs_8$  clusters are brought together. The ground-state geometries of  $VCs_9Cl$  and  $VCs_9I$  are shown in Supplementary Fig. S1b, and they are both stable species with halides that carry an extra charge. The direct combination of  $VCs_8$  yielded different results than that for  $VNa_8$ . Starting from a first  $VCs_8$ , a second  $VCs_8$  was brought towards the first unit from various initial directions and orientations. The lowest energy-optimized configuration is shown in Fig. 4b. The vanadium atoms did not come close enough to create a dimer, which was formed in the case of  $VNa_8$ , and were

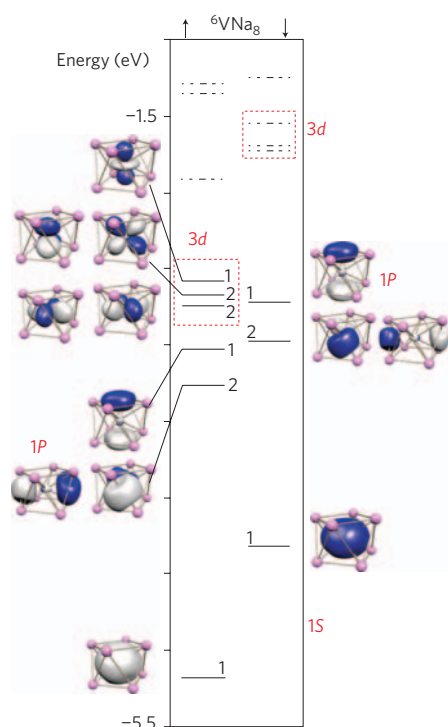


**Figure 3 | One-electron energy levels and molecular orbital charge density isosurfaces (isovalue 0.035 coulomb  $\text{m}^{-3}$ ) in the  $\text{VNa}_8$  cluster.** The majority and minority levels are shown. Continuous lines correspond to the filled levels and the dotted lines correspond to the unfilled states. For each level, the degeneracy is marked. Upper-case letters stand for delocalized 1S and 1P shells, and lower-case letters for localized 3d atomic orbitals.

separated by caesium atoms to form a  $(\text{VCs}_8)_2$  species, which indicates that the larger size of caesium atoms does prevent a collapse towards a  $(\text{V}_2\text{Cs}_{16})$  type of structure. More detailed investigations indicated a barrier of at least 0.3 eV against the formation of  $\text{V}_2\text{Cs}_{16}$  (a more stable structure) from separated  $\text{VCs}_8$  motifs.

The more interesting finding related to the magnetic state of  $(\text{VCs}_8)_2$ . The overall spin moment of  $(\text{VCs}_8)_2$  was  $12\mu_B$  and a closer analysis showed that the localized spins on the vanadium sites were ferromagnetically coupled with an antiferromagnetically coupled state that had 0.10 eV less energy. This has a commonality with atomic systems. For example, a manganese atom has an electronic configuration of  $d^5s^2$ , which corresponds to a filled  $d$  subshell and a filled  $s$  shell. In density functional theory the ground state of a  $\text{Mn}_2$  dimer has ferromagnetically coupled manganese moments<sup>19–21</sup>. For  $\text{VCs}_8$ , with a stability that originates in filled NFE shells, the finding of ferromagnetically coupled vanadium spins mimics the situation in a manganese atom. Further support for this analogy is given by a study of the effect of charging. For a  $\text{Mn}_2$  molecule, the difference between the ferromagnetic and antiferromagnetic configurations can be changed by removing an electron<sup>19–21</sup>. To explore similar effects in  $(\text{VCs}_8)_2$ , we calculated the lowest energy structure of the cation  $(\text{VCs}_8)_2^+$ . It was ferromagnetic with an overall spin moment of  $11\mu_B$ , with an antiferromagnetic solution only 0.066 eV higher in energy. Thus, charging the system favoured the antiferromagnetic state by decreasing the energy difference from 0.10 eV in the neutral case to 0.066 eV in the cationic system. Studies of a trimer of  $\text{VCs}_8$  superatoms  $(\text{VCs}_8)_3$  indicated an obtuse-angle triangular configuration, in which the magnetic moments of the vanadium atoms that form the longer side of the triangle are antiferromagnetically coupled to the central moment (see Supplementary Fig. S3). The net moment was  $5\mu_B$ . Also, in a  $\text{Mn}_3$  trimer, ferromagnetic and

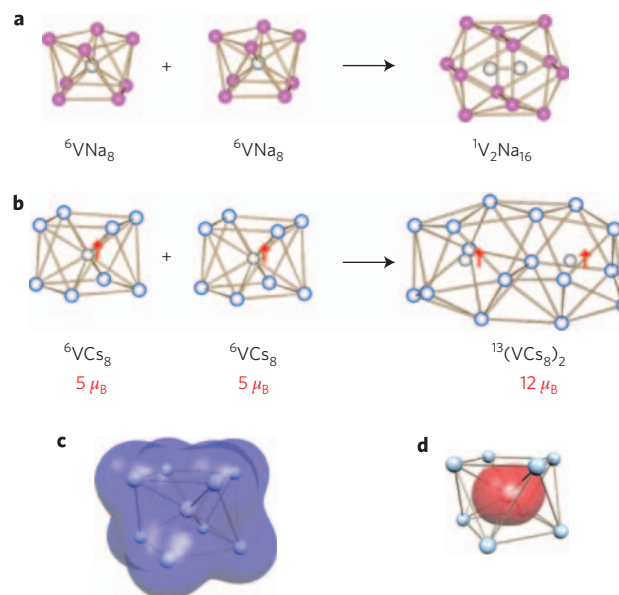


**Figure 4 | Lowest-energy structures of  $\text{V}_2\text{Na}_{16}$  and the  $(\text{VCs}_8)_2$  dimer, and total and net spin electron density of  $\text{VCs}_8$ .** **a,b**,  $\text{V}_2\text{Na}_{16}$  (**a**) and  $(\text{VCs}_8)_2$  dimer (**b**) starting from free clusters. The arrows indicate the direction of the vanadium local spin moments. The superscripts indicate spin multiplicity. **c,d**, Total electron density (**c**) and net spin electron density (isovalue 0.001 coulomb  $\text{m}^{-3}$ ) (**d**) in a  $\text{VCs}_8$  cluster. The spin density is mostly localized at the centre around the vanadium site.

frustrated antiferromagnetic solutions are found to be very close in energy within gradient-corrected density functional calculations<sup>19</sup>. We believe that  $\text{VCs}_8$  could be regarded as a magnetic superatom with localized  $d$  and diffuse  $SP$  shells, as confirmed by the spin and charge density in  $\text{VCs}_8$  shown in Fig. 4c,d. The spin density is almost entirely located on the vanadium site, whereas the total charge density is extended over the entire cluster.

As mentioned at the beginning of this article, the closures of the electronic shells in metallic clusters can be accomplished by attaching ligands that can withdraw electrons. This provides a unique opportunity to create stable magnetic superatoms using such ligated species. This is an exciting possibility because the outer ligands protect the central metallic core against interaction with other clusters. To demonstrate this unique prospect, we examined  $\text{Au}_{25}(\text{SCH}_3)_{18}^-$ , in which the central core of gold atoms has been shown to be particularly stable because of shell closure associated with eight  $SP$  valence electrons<sup>18,34</sup>. To form the magnetic superatom that maintained shell closure, we studied a neutral  $\text{MnAu}_{24}(\text{SH})_{18}$  cluster in which the central gold atom was replaced by a manganese atom in the anionic  $\text{Au}_{25}(\text{SCH}_3)_{18}^-$  cluster, the X-ray structure of which is available<sup>34</sup>. As the manganese atom contributes two  $s$  electrons, the neutral cluster is expected to maintain the shell closure, with the spin moment arising from localized  $d$  electrons of manganese. To keep the calculations of electronic structure manageable, the  $\text{SCH}_3$  groups were replaced by  $\text{SH}$  and the structure was fully optimized without symmetry constraints. Figure 5 shows the ground-state total electron density, the spin electron density and the density of electronic states. The theoretical studies, indeed, found a ground state with a net spin magnetic moment of  $5\mu_B$ . Detailed investigations revealed that the spin moment was localized at the manganese site (Fig. 5b). More importantly, the density of states (Fig. 5c) showed a closed electronic shell, with  $P$  states (green) closer to the Fermi energy, as observed in  $\text{Au}_{25}(\text{SCH}_3)_{18}^-$  (ref. 18) and  $\text{Au}_{25}(\text{SH})_{18}^-$  (ref. 34) clusters, which confirms a magnetic superatom with closure of the electronic shells rooted in  $s$  and  $p$  electrons!



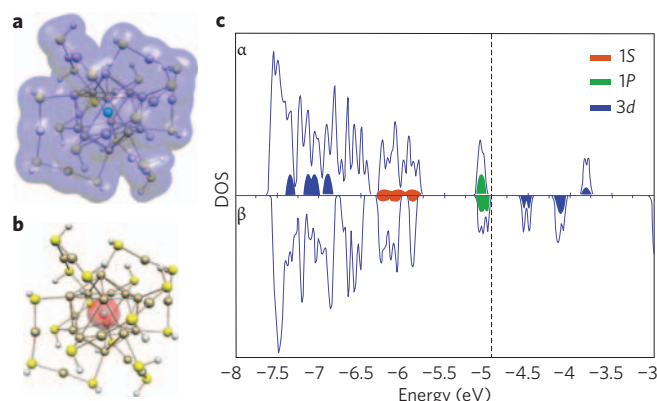


**Figure 5 | Total and net spin electron density and density of states (DOS) of the  $\text{MnAu}_{24}(\text{SH})_{18}$  cluster.** a–c, Total electron density (a), net spin electron density (isovalue  $0.01 \text{ e} \text{ Å}^{-3}$ ) (b) and DOS obtained by broadening the molecular levels by Gaussians of width  $0.017 \text{ eV}$  (c). Blue, gold, yellow and white circles represent, respectively, manganese, gold, sulfur and hydrogen atoms. The delocalized 1S and 1P electronic shells and localized 3d atomic orbitals are marked in orange, green and blue areas, respectively.

The present work shows that magnetic superatoms can be designed by appropriate combinations of localized and delocalized electrons in the valence space of a cluster, and offers  $\text{VNa}_8$ ,  $\text{VCs}_8$  and  $\text{MnAu}_{24}(\text{SH})_{18}$  as illustrative examples. The ligated magnetic superatoms may be expected to form molecular magnets with magnetic motifs that interact weakly, much as in  $\text{Mn}_{12}\text{O}_{12}$  acetate<sup>35</sup>. For free species,  $\text{VCs}_8$  mimics the magnetic behaviour of a manganese atom. There already exists overwhelming experimental evidence that vanadium impurities in alkali films carry large spin moments, which supports that  $\text{VCs}_8$  superatoms indeed carry large moments. The novelty offered by magnetic superatoms lies in that the localized spin moments coupled by shells of NFEs spread over alkali atoms (Fig. 4c). Here the coupling is weak and can be easily modulated. One area of interest is in molecular electronics for nanodevices. For example, the  $(\text{VCs}_8)_2$  supermolecule, marked by a small energy difference between the ferromagnetic and antiferromagnetic states, offers the possibility of changing the spin-polarized currents through the application of small fields<sup>36</sup>. Whereas the full potential of such applications will form the basis of future work, a preliminary density of states was obtained by broadening the molecular levels by Gaussians of width  $0.045 \text{ eV}$ . The majority spin density of states at the Fermi energy increases by almost 40% in going from the antiferromagnetic to the ferromagnetic state! Larger aggregation of such motifs is also likely to yield tunable materials. For example, our previous<sup>37</sup> and recent (unpublished) work on cluster assemblies based on metallic clusters with halide/alkali counterions shows that such assemblies are semiconductors in which the bandgap can be altered by changing the cluster or the counterion. We hope that this work to combine magnetism and semiconducting features that arise from a combination of motifs with filled shells will serve as the starting point for further systematic searches for such species.

## Methods

Calculations of the ground-state geometry, electronic structure and magnetic properties of  $\text{VNa}_n$ ,  $\text{VCs}_n$  and  $\text{MnAu}_{24}(\text{SH})_{18}$  clusters were carried out using a first-principles approach. The calculations used both the linear combination of atomic orbitals in a molecular orbital<sup>38–41</sup> and the plane-wave basis set approaches<sup>42–44</sup>, and were carried out within a gradient-corrected density functional formalism. Various functionals and numerical schemes were used to avoid uncertainty caused by the choice of the basis function, numerical procedure or density functional. For each cluster size, the ground-state configuration was obtained by starting from several initial configurations and moving the atoms in the direction of forces to minimize the energy. A frequency analysis was carried out to ascertain the stability

of the ground state and various spin configurations were attempted to find the ground state. Details of the theoretical procedures are provided in the Supplementary Information.

Received 21 January 2009; accepted 7 May 2009;  
published online 14 June 2009

## References

- Khanna, S. N. & Jena, P. Atomic clusters—building-blocks for a class of solids. *Phys. Rev. B* **51**, 13705–13716 (1995).
- Ashman, C. *et al.*  $(\text{BaI}_2)_n$  Cs: a cluster-assembled solid. *Phys. Rev. B* **55**, 15868–15875 (1997).
- Kumar, V. & Kawazoe, Y. Metal encapsulated icosahedral superatoms of germanium and tin with large gaps:  $\text{Zn@Ge}_{12}$  and  $\text{Cd@Sn}_{12}$ . *Appl. Phys. Lett.* **80**, 859–861 (2002).
- Neukermans, S. *et al.* Extremely stable metal-encapsulated  $\text{AlPb}_{10}^+$  and  $\text{AlPb}_{12}^+$  clusters. *Phys. Rev. Lett.* **92**, 163401 (2004).
- Bergeron, D. E., Castleman, A. W. Jr, Morisato, T. & Khanna, S. N. Formation of  $\text{Al}_{13}^-$ : evidence for the superhalogen character of  $\text{Al}_{13}^-$ . *Science* **304**, 84–87 (2004).
- Bergeron, D. E., Roach, P. J., Castleman, A. W. Jr, Jones, N. O. & Khanna, S. N. Al cluster superatoms as halogens in polyhalides and as alkaline earths in iodide salts. *Science* **307**, 231–235 (2005).
- Reveles, J. U., Khanna, S. N., Roach, P. J. & Castleman, A. W. Jr Multiple valence superatoms. *Proc. Natl Acad. Sci. USA* **103**, 18405–18410 (2006).
- Castleman, A. W. Jr *et al.* From designer clusters to synthetic crystalline nanoassemblies. *Nano Lett.* **7**, 2734–2741 (2007).
- Hartig, J., Stösser, A., Hauser, P. & Schnöckel, H. A metalloid  $[\text{Ga}_{23}\{\text{N}(\text{SiMe}_3)_2\}_{11}]$  cluster: the jellium model put to test. *Angew Chem. Int. Ed.* **46**, 1658–1662 (2007).
- Castleman, A. W. Jr & Khanna, S. N. Clusters, superatoms and building blocks of new materials. *J. Phys. Chem. C* **113**, 2664–2675 (2009).
- Knight, W. D. *et al.* Electronic shell structure and abundances of sodium clusters. *Phys. Rev. Lett.* **52**, 2141–2143 (1984).
- de Heer, W. A. The physics of simple metal clusters: experimental aspects and simple models. *Rev. Mod. Phys.* **65**, 611–676 (1994).
- Brack, M. The physics of simple metal clusters, self-consistent jellium model and semiclassical approaches. *Rev. Mod. Phys.* **65**, 677–732 (1993).
- Janssens, E., Neukermans, S. & Lievens, P. Shells of electrons in metal doped simple metal clusters. *Curr. Opin. Solid State Mater. Sci.* **8**, 185–193 (2004).
- Li, X., Wu, H., Wang, X.-B. & Wang, L.-S. *s-p* hybridization and electron shell structures in aluminum clusters: a photoelectron spectroscopy study. *Phys. Rev. Lett.* **81**, 1909–1912 (1998).
- Jadziński, P. D., Calero, G., Ackerson, C. J., Bushnell, D. A. & Kornberg, R. D. Structure of a thiol monolayer-protected gold nanoparticle at 1.1 Å resolution. *Science* **318**, 430–433 (2007).
- Walter, M. *et al.* A unified view of ligand-protected gold clusters as superatom complexes. *Proc. Natl Acad. Sci. USA* **105**, 9157–9162 (2008).
- Akola, J., Walter, M., Whetten, R. L., Hakkinen, H. & Gronbeck, H. On the structure of thiolate-protected  $\text{Au}_{25}$ . *J. Am. Chem. Soc.* **130**, 3756–3757 (2008).
- Pederson, M. R., Reuse, F. & Khanna, S. N. Magnetic transition in  $\text{Mn}_n$  ( $n = 2–8$ ) clusters. *Phys. Rev. B* **58**, 5632–5636 (1998).
- Desmarais, N., Reuse, F. A. & Khanna, S. N. Magnetic coupling in neutral and charged  $\text{Cr}_2$ ,  $\text{Mn}_2$ , and  $\text{CrMn}$  dimers. *J. Chem. Phys.* **112**, 5576–5584 (2000).
- Tzeli, D., Miranda, U., Kaplan, I. G. & Mavridis, A. First principles study of the electronic structure and bonding of  $\text{Mn}_2$ . *J. Chem. Phys.* **129**, 154310 (2008).
- Dorantes-Davila, J. & Dreyse, H. Magnetic behavior of small vanadium clusters. *Phys. Rev. B* **47**, 3857–3863 (1993).
- Song, F. & Bergmann, G. Strongly enhanced magnetic moments of vanadium impurities in thin films of sodium and potassium. *Phys. Rev. Lett.* **88**, 167202 (2002).
- Bergmann, G. & Song, F. Electronic transition of vanadium impurities in different alkali hosts. *J. Magn. Magn. Mater.* **272**, E863–E864 (2004).
- Sahu, B. R. & Kleinman, L. Nonenhancement of magnetic moments on transition metal impurities by alkali metal hosts. *Phys. Rev. B* **67**, 094424 (2003).
- Pradhan, K., Sen, P., Reveles, J. U. & Khanna, S. N. First principles study of Sc, Ti, and V doped  $\text{Na}_n$  ( $n = 4, 5, 6$ ) clusters: enhanced magnetic moments. *Phys. Rev. B* **77**, 045408 (2008).
- Gong, X. G. & Zheng, Q. Q. Electronic structures and stability of  $\text{Si}_{60}$  and  $\text{C}_{60}@\text{Si}_{60}$  clusters. *Phys. Rev. B* **52**, 4756–4759 (1995).
- Sattler, K. (ed.) *Cluster Assembled Materials* (Trans Tech Publications, 1996).
- Perez, A. *et al.* Cluster assembled materials: a novel class of nanostructured solids with original structures and properties. *J. Phys. D* **30**, 709–721 (1997).
- Jena, P., Khanna, S. N. & Rao, B. K. (eds) *Clusters and Nano-Assemblies* (World Scientific, 2003).
- Mikhailov, M. N., Kustov, L. M. & Kazansky, V. B. The state and reactivity of  $\text{Pt}_6$  particles in ZSM-5 zeolite. *Catal. Lett.* **120**, 8–13 (2008).
- Khanna, S. N. & Jena, P. Designing ionic solids from metallic clusters. *Chem. Phys. Lett.* **219**, 479–483 (1994).

33. Reber, A. C., Khanna, S. N. & Castleman, A. W. Jr Superatom compounds, clusters, and assemblies: ultra alkali motifs and architectures. *J. Am. Chem. Soc.* **129**, 10189–10194 (2007).
34. Zhu, M., Aikens, C. M., Hollander, F. J., Schatz, G. C. & Jin, R. Correlating the crystal structure of a thiol-protected Au cluster and optical properties. *J. Am. Chem. Soc.* **130**, 5883–5885 (2007).
35. Sessoli, R., Gatteschi, D. & Wernsdorfer, W. Quantum tunneling of the magnetization in molecular nanoclusters in *Quantum Phenomena in Clusters and Nanostructures* (eds Khanna S. N. & Castleman, A. W. Jr), 55–79 (Springer, 1993).
36. Zimbovskaya, N. A. & Pederson, M. R. Negative differential resistance in molecular junctions: effect of the electronic structure of the electrodes. *Phys. Rev. B* **78**, 153105 (2008).
37. Ashman, C., Khanna, S. N., Pederson, M. R. & Kortus, J.  $\text{Al}_7\text{CX}$  ( $X = \text{Li} - \text{Cs}$ ) clusters: stability and the prospect for cluster materials. *Phys. Rev. B* **62**, 16956–16961 (2000).
38. Koster, A. M. *et al.* deMon2 k, V. 2.3.6 (The deMon Developers Community, Cinvestav, México, 2006).
39. Pederson, M. R. & Jackson, K. A. Variational mesh for quantum-mechanical simulations. *Phys. Rev. B* **41**, 7453–7461 (1990).
40. Jackson, K. & Pederson, M. R. Accurate forces in a local-orbital approach to the local-density approximation. *Phys. Rev. B* **42**, 3276–3281 (1990).
41. Porezag, D. & Pederson, M. R. Optimization of Gaussian basis sets for density-functional calculations. *Phys. Rev. A* **60**, 2840–2847 (1999).
42. Kresse, G. & Furthmüller, F. Efficient iterative schemes for *ab initio* total-energy calculations using a plane-wave basis set. *Phys. Rev. B* **54**, 11169–11186 (1996).
43. Kresse, G. & Furthmüller, F. Efficiency of *ab-initio* total energy calculations for metals and semiconductors using a plane-wave basis set. *Comp. Mater. Sci.* **6**, 15–50 (1996).
44. Kresse, G. & Joubert, D. From ultrasoft pseudopotentials to the projector augmented-wave method. *Phys. Rev. B* **59**, 1758–1775 (1999).

### Acknowledgements

We gratefully acknowledge support from the US Department of the Army through a MURI grant. Parts of the computations were performed at the cluster computing facility at the Harish-Chandra Research Institute, and on the computational equipment of La Dirección General de Servicios de Cómputo Académico de la Universidad Nacional Autónoma de México, particularly at the super computer KanBalam.

### Author contributions

All the authors discussed the results and commented on the manuscript.

### Additional information

Supplementary information accompanies this paper at [www.nature.com/naturechemistry](http://www.nature.com/naturechemistry). Reprints and permission information is available online at <http://npg.nature.com/reprintsandpermissions/>. Correspondence and requests for materials should be addressed to S.N.K.